Oscillation spectra of semilinear photorefractive coherent oscillator with two pump waves

Pierre Mathey

Laboratoire de Physique, Université de Bourgogne, BP 47870, 21078 Dijon, France

Serguey G. Odoulov

Institute of Physics, National Academy of Sciences, 03650, Kiev-39, Ukraine

Daniel Rytz

Forschunginstitute fur mineralische und metalische Werkstoffe, Edelsteine/Edelmetalle GmBH, Struhtstrasse 2, Wackenmuhle, 55743 Idar-Oberstein, Germany

Received April 4, 2002; revised manuscript received June 26, 2002

The transition of the single-frequency oscillation of a semilinear photorefractive coherent oscillator for sufficiently large coupling strengths into two-frequency oscillation is predicted and is observed experimentally. The critical value of coupling strength at which the bifurcation occurs is a function of pump-intensity ratio and cavity losses. For certain combinations of these parameters, the critical coupling strength for spectrum bifurcation becomes smaller than the threshold coupling strength: in these cases double-frequency oscillation appears at the threshold. The supercritical bifurcation in the oscillation spectrum is analogous to the second-order phase transition. © 2002 Optical Society of America

OCIS codes: 190.4380, 190.5040, 190.5330, 230.4910.

1. INTRODUCTION

A semilinear coherent oscillator with two pump waves[1] was the very first coherent oscillator with a photorefractive crystal as the gain medium.[2] Its cavity is formed by an ordinary mirror and a photorefractive crystal that serves as an amplifying phase-conjugate mirror when being pumped with two counterpropagating pump waves. This configuration of a photorefractive oscillator attracts attention because of potential applications in lasers with capability for intracavity phase-distortion compensation.[3,4] It served also as a model system for investigation of deterministic chaos.[5,6] The onset of coherent oscillation in this geometry, as it has been shown recently, is similar to the second-order phase transition.[7,8]

In all publications mentioned above, the frequency-degenerate oscillation was considered except in Ref. 6, where the authors report on excitation of the high-index transverse modes that might be frequency shifted with respect to the pump waves. Although most often the frequency of output radiation in photorefractive oscillators with unclosed cavities coincides with the frequency of the pump radiation, this is not imposed by any general law. As in usual lasers, in coherent oscillators the cavity modes that oscillate should possess the largest gain and smallest losses; nothing indicates in advance that this must necessarily be the mode with the pump frequency.

In this paper we present the results of calculations that predict a bifurcation in the oscillation spectrum of a semilinear coherent oscillator, within the plane-wave approximation, i.e., even for the lowest-index transverse modes. This prediction is further confirmed experimentally, when studying a semilinear photorefractive oscillator with $BaTiO_3$.

Above the oscillation threshold, a photorefractive grating self-develops in the sample, which couples the oscillation waves to the pump waves. The splitting of the single line in the oscillation spectrum into two symmetric lines means that a single immobile refractive-index grating below the bifurcation point is replaced above the bifurcation point by two gratings with the same grating vector but moving in opposite directions with the same speed. The transition between these two ordered states (immobile grating and moving grating) can be considered as a type of phase transition that has no direct analogy in solid-state physics. It is shown that the splitting in the oscillation spectrum features properties of the second-order phase transitions.

2. QUALITATIVE DESCRIPTION

The oscillator geometry shown in Fig. 1 is considered. The photorefractive crystal (PRC) is illuminated with two counterpropagating pump waves, 1 and 2. Any noisy wave propagating in direction 4 (part of the pump radiation scattered from optical imperfections of the sample) gives rise to phase-conjugate wave 3, i.e., the photorefractive crystal serves as a phase-conjugate mirror. The ratio of intensities of the wave 3 to wave 4 at the input face $z = 0$ (see Fig. 1) is called phase-conjugate reflectivity, R_{pc}. A conventional mirror M with reflectance R serves

0740-3224/2002/122967-11$15.00

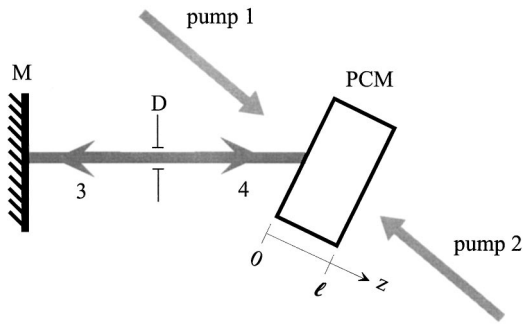

Fig. 1. Schematic representation of the considered oscillator. The oscillator consists of a four-wave mixing phase-conjugate mirror, PCM, and a conventional mirror, M; the aperture D is placed inside the cavity to reduce its Fresnel number to be $N_F \simeq 1$. Pump waves are labeled 1 and 2, and 3 and 4 define the oscillation wave.

as the second cavity mirror. The aperture D is introduced inside the cavity, with the diameter a that ensures the cavity Fresnel number close to unity, $N_F = a^2/\lambda L \simeq 1$ (λ is the light wavelength, and L is the distance between the phase-conjugate mirror and the conventional mirror). In such a way, the lowest index transverse mode is selected.

The steady-state oscillation occurs if the intensity of the oscillation wave remains the same after one round trip inside the cavity, which leads to condition

$$R_{\mathrm{pc}} R = 1. \tag{1}$$

In the undepleted-pump approximation, the phase-conjugate reflectivity reads[3]

$$R_{\mathrm{pc}} = \frac{\sinh^2\left(\frac{\gamma_0 \ell}{2}\right)}{\cosh^2\left(\frac{\gamma_0 \ell}{2} - \frac{\ln r}{2}\right)}, \tag{2}$$

where γ_0 is the coupling constant, ℓ is the interaction length, and $r = I_2(\ell)/I_1(0)$ is the pump-intensity ratio.

For frequency-degenerate interaction with the pump ratio

$$r = \exp(\gamma_0 \ell), \tag{3}$$

optimized to reach the highest phase-conjugate reflectivity, Eq. (2) reduces to $R_{\mathrm{pc}} = \sinh^2(\gamma_0 \ell/2)$ and predicts, for high-enough coupling strengths, an exponential growth of the phase-conjugate reflectivity $R_{\mathrm{pc}} \simeq [\exp(-\gamma_0 \ell)]/4$. In this way Eq. (1) takes the form

$$\exp(-\gamma_0 \ell) \approx 4/R. \tag{4}$$

With $-\ln(R)$ being the dimensionless losses because of mirror transparency the oscillation condition becomes

$$(-\gamma_0 \ell)_{\mathrm{th}} = -\ln(R) + \ln 4. \tag{5}$$

Equation (5) resembles, to a certain extent, the oscillation condition for conventional lasers, which says that, to get the oscillation, the exponential gain should compensate for all types of cavity losses. The necessity to ensure R_{pc} at least larger than unity to achieve the oscillation leads to the additional term, $\ln 4$, on the right-hand side of Eq. (5).

There are several other fundamental differences between this photorefractive coherent oscillator and conventional lasers. The semilinear geometry belongs to the oscillators with so-called unclosed cavities. After every round trip in the cavity, the photons of the oscillation wave leave the cavity forever, new photons being permanently supplied by the diffraction of the pump wave from the photorefractive grating. In other words, the phase-conjugate mirror does not return the photons of the oscillation wave back to the cavity but injects all the time new photons. The resonant frequencies of the cavity with the phase-conjugate mirror are not fixed,[9,10] and the oscillation may occur at any frequency imposed by the threshold conditions (i.e., by the spectra of gain and losses).

A next distinction lies in the description that represents the coherent oscillator as the system with localized gain (phase-conjugate mirror) and localized losses (ordinary mirror), whereas conventional lasers are usually treated as systems with distributed gain (medium with inverted population) and either localized or distributed losses. The fact that coupling strength in Eqs. (3) and (4) is a product of the coupling constant γ_0 times the crystal thickness ℓ might be misleading here: one should remember, however, that the sample thickness ℓ appears only because it defines R_{pc} in Eq. (1), i.e., the intensity ratio of the wave "reflected" from the phase-conjugate mirror and the wave incident at its input face $z = 0$; see Fig. 1.

The important distinction also is that the gain in the cavity with the phase-conjugate mirror depends not only on coupling strength but also on the pump-intensity ratio. Up to now we have discussed the optimum case when the pump ratio is related to the coupling strength through Eq. (3), but in fact these are two independent control parameters for a photorefractive oscillator. As the coupling strength is usually intensity independent in photorefractive crystals, r and R remain two suitable control parameters for the experiment.

The exact solution for the intensity of the oscillation wave within the assumption of frequency-degenerate interaction of four plane waves is presented in Ref. 8, with pump depletion taken into account. Referring to these results, we are reminded that in the vicinity of the threshold the normalized amplitude of the oscillation wave $|E_3(0)/E_2(0)| = \sqrt{I_3(0)/I_2(0)}$ features supercritical bifurcation,[11,12]

$$\left|\frac{E_3(0)}{E_2(0)}\right| \approx A \sqrt{\frac{(\gamma_0 \ell) - (\gamma_0 \ell)_{\mathrm{th}}}{(\gamma_0 \ell)_{\mathrm{th}}}}, \tag{6}$$

with

$$(\gamma_0 \ell)_{\mathrm{th}} = \ln \frac{\sqrt{rR} - 1}{\sqrt{r}(\sqrt{R} + \sqrt{r})}, \tag{7}$$

A being a constant independent of $(\gamma_0 \ell)_{\mathrm{th}}$. The latter suggests the analogy of the oscillation threshold to the second-order phase transition.[8]

We describe below the calculations where the oscillation frequency is not imposed to be equal to the pump frequency (nondegenerate case). Assuming that the cavity losses are frequency independent, the oscillation frequen-

cies are determined from the position of the maxima of the phase-conjugate reflectivity spectra[13,14] exactly at threshold.

3. CALCULATION OF OSCILLATION FREQUENCIES

The same condition of oscillation [Eq. (1)] is considered, with low-signal phase-conjugate reflectivity given by Eq. (2), which is well justified at the threshold of oscillation. The distinction is that the oscillation wave is allowed to be shifted in frequency to Ω with respect to the pump waves, i.e., $\omega_1 = \omega_2 = \omega$, whereas $\omega_3 = \omega \pm \Omega$ and $\omega_4 = \omega \mp \Omega$. It is known[9,10] that, being reflected from the considered phase-conjugate mirror, the light wave with frequency $(\omega + \Omega)$ acquires frequency $(\omega - \Omega)$ and vice versa. This is one of the reasons why the oscillation wave is self-reproduced only after two full round trips in the cavity, as distinct from conventional lasers where one round trip is sufficient. Therefore for the nondegenerate case, the oscillation wave should always contain two components, shifted symmetrically by $\pm\Omega$ with respect to the pump frequency.

The coupling constant that becomes a complex value due to the possible frequency shift of the oscillation wave reads

$$(\gamma\ell) = \frac{\gamma_0\ell}{1 + \tau^2\Omega^2} + i\tau\Omega\frac{\gamma_0\ell}{1 + \tau^2\Omega^2} = (\gamma''\ell) + i(\gamma'\ell), \tag{8}$$

where γ_0 is the initial *real* coupling constant that characterizes the diffusion-mediated photorefractivity with nonlocal response (e.g., $BaTiO_3$). The grating relaxation time τ is equal, in the zeroth approximation, to dielectric relaxation time $\tau_{di} = \epsilon\epsilon_0/\sigma$, where $\epsilon\epsilon_0$ is the dielectric constant and σ is the photoconductivity, $\sigma = \kappa I$, with κ being the specific photoconductivity. With Eq. (8) taken into account, the phase-conjugate reflectivity becomes

$$R_{pc} = \frac{\sinh^2\left(\frac{\gamma''\ell}{2}\right) + \sin^2\left(\frac{\gamma'\ell}{2}\right)}{\cosh^2\left(\frac{\gamma''\ell - \ln r}{2}\right) - \sin^2\left(\frac{\gamma'\ell}{2}\right)}. \tag{9}$$

It is now a function of frequency detuning because both γ'' and γ' depend on Ω.

The aim of the calculation is to find the oscillation frequencies Ω_{th} at the threshold of oscillation and threshold values of coupling strength $(\gamma_0\ell)_{th}$ for different pump ratios r and end-mirror reflectivities R. To do it, the set of equations should be solved:

$$R_{pc}R = 1, \tag{10a}$$

$$\frac{dR_{pc}}{d\Omega} = 0, \tag{10b}$$

with R_{pc} given by Eqs. (9) and (8). The reflectivity R of the end mirror is considered to be independent of frequency detuning Ω. The second equation, Eq. 10(b), allows us to interrelate the variables $(\gamma_0\ell)$, r, and Ω at the maxima of phase-conjugate reflectivity:

$$\frac{d(\gamma''\ell)}{d\Omega}\left[-2\sin^2\left(\frac{\gamma'\ell}{2}\right)\sinh\left(\gamma''\ell - \frac{\ln r}{2}\right)\right] + 2\sinh\left(\frac{\gamma''\ell}{2}\right)\cosh\left(\frac{\gamma''\ell - \ln r}{2}\right)\Bigg] = -\frac{d\gamma'\ell}{d\Omega}\sin(\gamma'\ell)\cosh\left(\gamma''\ell - \frac{\ln r}{2}\right). \tag{11}$$

To solve this equation together with the threshold condition, Eq. (10a), the numerical simulations are used; only some particular cases can be treated analytically.

Before presenting the summary of the numerical simulations, some representative examples are shown and two limiting cases are analyzed. We first impose constant pump ratio $r = 2$ and vary coupling strength. For coupling strength $\gamma_0\ell = -1$, the phase-conjugate reflectivity spectrum has only one maximum with R_{pc} smaller than unity (curve 1 in Fig. 2); therefore the oscillation does not occur. With $\gamma_0\ell = -2.1$, the phase-conjugate reflectivity spectrum still has only one maximum, but $R_{pc} = 1$ is reached (curve 2). This means that oscillation in cavity with high-reflecting end mirror $R = 1$ will start with only one frequency at the threshold. With larger coupling strength $\gamma_0\ell = -3$, the phase-conjugate reflectivity spectrum has two maxima, and the threshold of oscillation can be reached in the cavity with a mirror reflectivity $R \simeq 0.53$ (curve 3). Increasing further the coupling strength to $\gamma_0\ell = -5$, we see that the oscillation condition can be satisfied in the cavity with a mirror reflectivity $R \simeq 0.23$ (curve 4).

It should be emphasized here that the appearance of two maxima in the spectrum of phase-conjugate reflectivity is a consequence of parametric mixing of four light waves; the spectrum of the gain factor $\Gamma = 2\gamma''$ always has the Lorentzian shape given by Eq. (8).

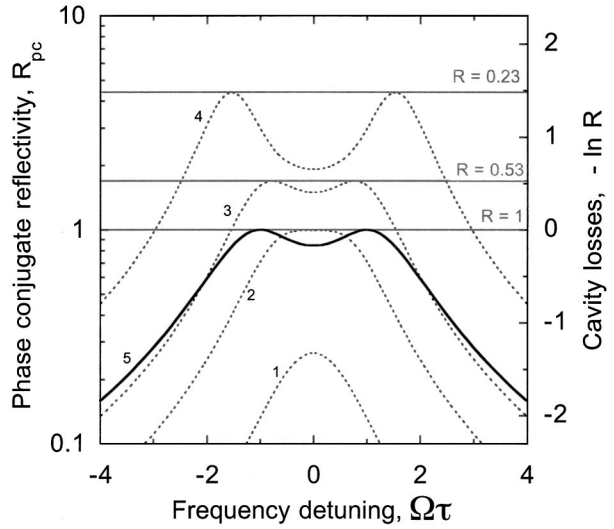

Fig. 2. Spectra of phase-conjugate reflectivity (black dashed and solid curves) and cavity losses (horizontal gray lines) that show the threshold condition of oscillation. Coupling strength is equal to -1 (curve 1), -2.1 (curve 2), -3 (curve 3), -5 (curve 4), and $-\pi$ (curve 5). Pump ratio r is equal to 2 for all dashed curves and 1 for the black solid curve. The mirror reflectivities are indicated near the horizontal lines, depicting loss levels.

Let us suppose that the two pump waves have identical intensities, $r = 1$, and that the cavity has a highly reflecting mirror, $R = 1$. It is easy to deduce from Eq. (2) that in the frequency-degenerate case the phase-conjugate reflectivity becomes $R_{pc} = \tanh^2(\gamma_0 \ell/2)$; i.e., it approaches unity only for an infinitely large coupling strength. As a result, we come to the known conclusion that the frequency-degenerate coherent oscillation is impossible with $r = 1$, even in lossless cavity ($R = 1$). This becomes not true, however, if frequency degeneracy is removed. It appears that Eq. (10) with $R = 1$ and $r = 1$ can be satisfied if

$$2 \sin^2(\gamma' \ell/2) = 1, \tag{12a}$$

$$\left[\frac{d(\gamma'' \ell)}{d\Omega}\right] \tanh(\gamma'' \ell) = -\left[\frac{d(\gamma' \ell)}{d\Omega}\right] \tan(\gamma' \ell). \tag{12b}$$

Equation (12a) leads to $(\gamma' \ell) = \pm(\pi/2) + p\pi$, where p is an integer. By putting this on the right-hand side of Eq. (12b) and taking into account that the left-hand side of this equation remains finite, we need to impose $\Omega = \pm 1$ to satisfy Eq. (12b). In turn, this gives the coupling strength $(\gamma_0 \ell)_{th} = -\pi$. This example shows that frequency-nondegenerate oscillation may occur for the set of parameters where it is forbidden in the degenerate case, and it shows that the coherent oscillation in a low-loss cavity ($R = 1$) can be reached for the set of parameters other than that for curve 2 in Fig. 2; see solid curve 5 in Fig. 2.

The other limiting case is the mirrorless oscillation that is supposed to appear if the conventional cavity mirror is removed, $R = 0$, i.e., if R_{pc} tends to infinity. The latter happens if the denominator of the right-hand part of Eq. (9) becomes zero:

$$\cosh^2\left(\frac{\gamma'' \ell - \ln r}{2}\right) = \sin^2(\gamma' \ell/2), \tag{13}$$

which leads to conditions

$$\Omega_{th}^{ml} = \frac{\pi}{\ln r}, \tag{14}$$

$$(\gamma_0 \ell)_{th}^{ml} = -\ln r \left[1 + \left(\frac{\pi}{\ln r}\right)^2\right], \tag{15}$$

where superscript ml marks mirrorless oscillation. Qualitatively, this result is in agreement with the conclusion of Ref. 3, which predicted mirrorless oscillation for media with a mixed local/nonlocal nonlinear response; in other words, for media with complex coupling strength.

Figure 3 shows the pump-ratio dependences given by Eqs. (14) and (15). The lowest threshold of mirrorless oscillation $(\gamma_0 \ell)_{th}^{ml} = -2\pi$ and $\Omega_{th}^{ml} = 1$ are reached for $r = \exp(\pi) \approx 23.14$. This allows us to conclude that the mirrorless oscillation can be achieved in $BaTiO_3$ samples with reasonable dimensions.

Below, the pump-ratio dependences of $(\gamma_0 \ell)_{th}$ and Ω_{th} are calculated numerically from Eqs. (10a) and 10(b) for cavity mirrors with different reflectances. The results are presented in Fig. 4. They include also the analytical solutions for the limiting cases described above. One can see from the data presented in Fig. 4B that for any particular R there exists a certain critical value of pump ratio r_{cr} below which the single line in the oscillation spectrum bifurcates into two lines symmetric with respect to the pump frequency (only one, positive branch is shown in Fig. 4B because a log plot is used). Within the interval of the pump ratio where the oscillation spectrum possesses a

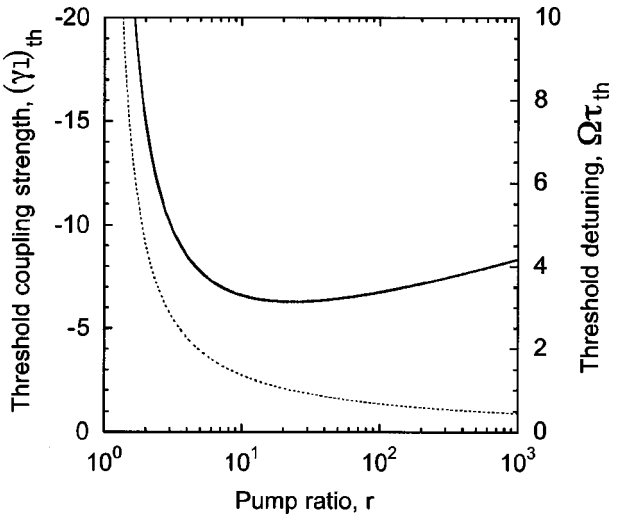

Fig. 3. Calculated pump-ratio dependences of the threshold-coupling strength (solid curve) and threshold frequency detuning (dashed curve) for the mirrorless coherent oscillation.

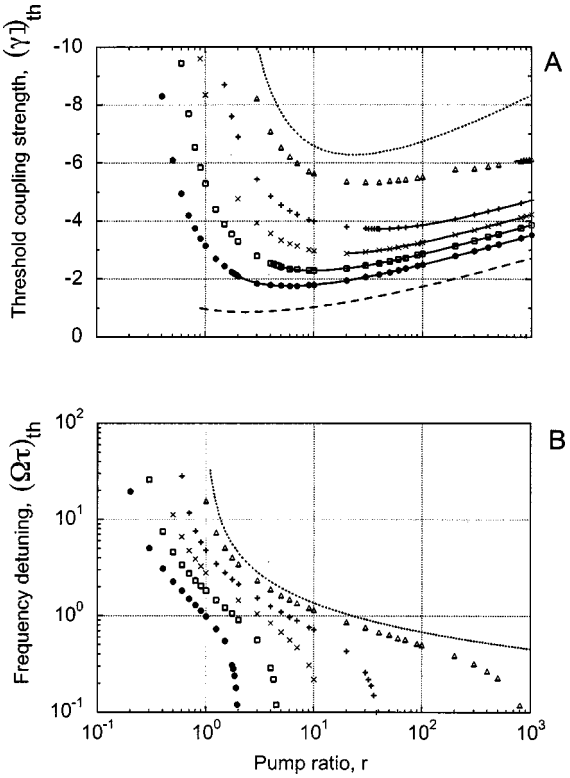

Fig. 4. Calculated pump-ratio dependences of (A) the threshold coupling strength and (B) the threshold frequency detuning for the coherent oscillation in a semilinear cavity. Cavity mirror reflectivity $R = 1$ for filled dots, 0.5 for diamonds, 0.25 for slanted crosses, 0.1 for straight crosses, 0.01 for triangles, 0 for the dotted curve (mirrorless oscillation), and 5 for the dashed curve (oscillation with amplifier inside the cavity). Solid curves in (A) represent an analytical solution for single-frequency oscillation.

single frequency, the threshold coupling strength can be calculated from Eq. (7). Solid curves in Fig. 4A show the results. A good agreement with the numerical calculations is obvious, which proves the validity of the numerical calculations for the whole range of r values investigated.

The detailed analysis in the close vicinity of the critical pump ratio shows (see Fig. 5) that below r_{cr} the threshold frequency Ω_{th} is reasonably well described by a square-root dependence,

$$\Omega_{th} \simeq B \sqrt{\frac{\ln r_{cr} - \ln r}{\ln r_{cr}}}, \tag{16}$$

where B is constant, i.e., the splitting occurs by supercritical bifurcation.[11,12]

The smaller the cavity mirror reflectivity is, the larger value of r is needed to get single-frequency oscillation. Inevitably, this is accompanied by the increase of the threshold coupling strength. The smallest coupling strength needed to reach the bifurcation in a low-loss cavity goes to $(\gamma_0\ell)_{cr} \approx -1.7$ (see Fig. 4A). Even lower values are possible in case the conventional laser amplifier is put inside the cavity. As an example, the dashed curve is shown in Fig. 4A for an effective mirror reflectivity $R = 5$. Altogether, the data of Fig. 4 lead to the conclusion that the double-frequency oscillation is quite natural for a semilinear coherent photorefractive oscillator with two pump waves and should be easily observed in the experiment.

Figure 6 represents a two-dimensional "phase diagram" (coupling strength and pump ratio) that shows the white area where oscillation is impossible without extra amplifiers; the area of existence of single-frequency oscillation is marked by light gray color, and the area of possible excitation of double-frequency oscillation is marked by deeper gray color

The solid black curve separating the white area from filled areas defines the smallest threshold of oscillation in lossless cavity ($R = 1$) as a function of r (curve taken from Fig. 4B). The vertical solid straight line indicates the smallest pump ratio r below which the oscillation occurs with two frequencies even at threshold. The tilted straight line represents the condition $\gamma''\ell = \ln r$ that optimizes R_{pc} in the nondegenerate case. At last, the dotted curve that defines the border of the deep-gray area in Fig. 6 shows the coupling strength that corresponds to the bifurcation in the frequency spectrum. This dependence is found from the condition

$$\frac{d^2 R_{pc}}{d^2 \Omega} = 0, \tag{17}$$

supplemented with the condition given by Eq. (10b). These two equations give the relationship between $\gamma_0\ell$ and r:

$$r = \frac{\gamma_0\ell \exp(\gamma_0\ell) + 2[1 - \exp(\gamma_0\ell)]}{-\gamma_0\ell \exp(-\gamma_0\ell) + 2[1 - \exp(-\gamma_0\ell)]}. \tag{18}$$

Note that the condition of oscillation [Eq. (10a)] has not been explicitly used in this calculation: It is supposed that R is changing along with changing r in such a manner that Eq. (10a) is permanently satisfied.

One can see from Fig. 4A that the solutions for different R are not intersecting each other; i.e., for every set of r and R, only one $(\gamma_0\ell)_{th}$ can be found. At the same time, the absolute minimum of the threshold-coupling strength for gradually decreasing R has a multivalued region when plotted as a function of pump ratio (Fig. 6, diamonds). It might be expected that this absolute minimum can be found from the condition $\gamma''\ell = \ln r$ that optimizes R_{pc} in the nondegenerate case (tilted straight solid line in Fig. 6), but this proves to be true only within the limited interval of r where optimum conditions correspond to single-frequency oscillation. When the coupling strength necessary for frequency splitting becomes smaller than that given by the condition $\gamma''\ell = \ln r$, the absolute minimum in threshold-coupling strength strongly deviates from $\gamma''\ell = \ln r$ dependence.

To this point, we have discussed the dependences of $(\gamma_0\ell)_{th}$ and Ω_{th} on pump-intensity ratio r. The other possible control parameter to observe the frequency splitting

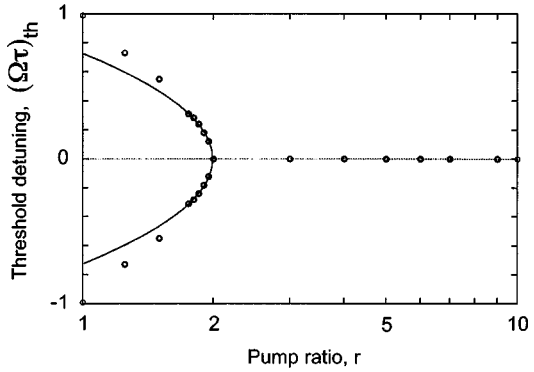

Fig. 5. Calculated pump-ratio dependence of the threshold frequency detuning for coherent oscillation with a high-reflecting ($R = 1$) cavity mirror in the vicinity of the bifurcation point. The curve shows the fit to a square-root dependence of Eq. (16).

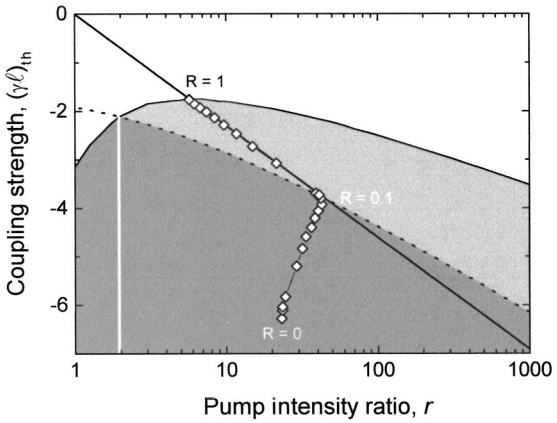

Fig. 6. Two-dimensional diagram of coherent oscillation existence. Light-gray color defines the area where only single-frequency oscillation is possible, and deep-gray color marks areas where both single-frequency and double-frequency oscillation may occur, depending on cavity losses. For pump ratios smaller than that indicated by a white straight line, only double-frequency oscillation can be excited. Diamonds show the pump-ratio dependence of the smallest threshold coupling strength for different cavity mirror reflectivities. The tilted straight line represents the coupling strength that optimizes the phase-conjugate reflectivity for a frequency-degenerate oscillation.

in this photorefractive oscillator is the cavity mirror reflectivity R. With the data of Fig. 4B redrawn to show the dependences of $(\gamma_0 \ell)_{\mathrm{th}}$ and Ω_{th} versus $\ln R$, the same type of subcritical bifurcation is revealed in the frequency spectrum as that shown in Fig. 5.

4. EXPERIMENT

A. Experimental Technique

The semilinear oscillator depicted schematically in Fig. 7 consists of a phase-conjugate mirror in a cobalt-doped photorefractive barium titanate PRC and a conventional highly reflecting convex mirror M_c with a 50-cm radius of curvature. The distance between the mirror and the crystal is 38 cm; the 0.5-mm aperture is placed ~12 cm from the conventional mirror.

The Ar^+-laser beam (514 nm, TEM_{00}, no etalon) is loosely focused by the lens L_1, with 100-cm focal length, into the sample (the distance between the sample and lens is 90 cm). A beam splitter BS, which divides the incident beam into two beams with the intensity ratio 3:1, and two flat highly reflecting mirrors M_1 and M_2 are used to form counterpropagating pump waves 1 and 2. The polarizing prism P and a $\lambda/2$ phase retarder between the mirrors M_1 and M_2 serve to change pump-intensity ratio by decreasing the intensity of a weak backpropagating pump wave. Both pump waves are polarized in a way to be extraordinary waves in the $BaTiO_3$ sample. A Faraday isolator is placed close to the Ar^+-laser output mirror to prevent undesirable feedback to the pump laser from the coherent oscillator. If not specified, the used output power of the Ar^+-laser is ~250 mW.

An Ar^+ laser with a short coherence length is selected as a pump source in these experiments deliberately to prevent the direct recording of the reflection gratings. Special care is taken to ensure the smallest possible path difference between the oscillation wave sent to the sample from mirror M_c and copropagating pump wave 1. In such a way, the recording of the transmission gratings only is favored.

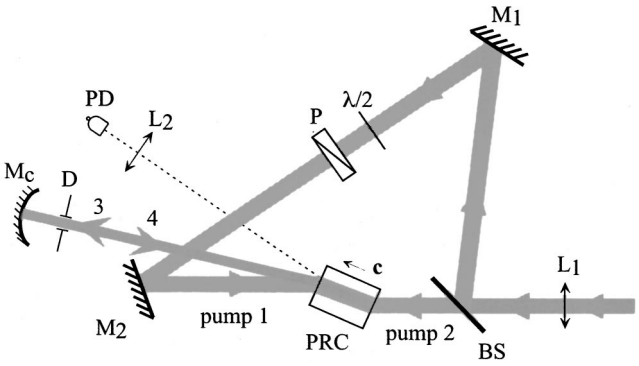

Fig. 7. Experimental arrangement for the study of coherent oscillation in a semilinear cavity. Beam splitter BS and mirrors M_1 and M_2 form two counterpropagating pump beams that impinge upon the $BaTiO_3$ sample (PRC). M_c is a highly reflecting conventional convex mirror, D is a diaphragm, and L_2 is a lens that collects the oscillation light (reflected from the sample face closest to the beam splitter) and sends it to photodetector PD. The polarizer P and half-wave phase retarder $\lambda/2$ serve to control the intensity of pump wave 1. The Faraday optical isolator (not shown in this picture) is put between the argon laser and beam splitter.

The $BaTiO_3$:Co sample has 3.7 mm 4.0 × mm × 6.1 mm dimensions along X, Y, and Z crystallographic directions. The pump waves enter the sample from two opposite faces normal to the polar ferroelectric axis (c axis); the sample is aligned in a way that backscattered waves from pump 1 are amplified. To increase the coupling strength for copropagating waves 2 and 3, the pump-incidence angle is chosen to be 32° in air, and the angle that the optical-cavity axis makes with the crystal c axis is 8°. The coupling strength estimated for $BaTiO_3$ ($n_e \approx 2.488$, $n_o \approx 2.424$, $r_{42} = 1640$ pm/V), according to the procedure described in Refs. 15 and 16, should be 7, i.e., is sufficient for the observation of frequency splitting with cavity oscillation and for the detection of mirrorless oscillation.

When the oscillation is achieved, a part of it is reflected from the sample faces; this light is focused by the lens L_2 to the detector PD to measure the oscillation dynamics. In some experiments, a part of this oscillation beam is used to form the fringe pattern together with the reference beam from the Ar^+ laser to measure the frequency detuning from the beat-frequency mark. The path difference between the oscillation and reference waves is minimized to obtain high-contrast moving fringes.

B. Oscillation in Semilinear Cavity

When the aperture is removed from the cavity, several modes with high transverse indices are oscillating simultaneously and/or changing each other, and the temporal dynamics of the oscillation wave is irregular. This is in agreement with the results reported in Ref. 6, especially taking into account the higher coupling strength in our experiment as compared with that in Ref. 6.

The onset of oscillation is similar to that already described for other photorefractive coherent oscillators (e.g., double phase-conjugate mirror[17] or ring-loop oscillator[18]): After the beginning of exposure of the virgin sample to pump waves, the intensity of the future oscillation wave remains for a certain time very small and then is increasing nonlinearly, quickly reaching its saturation level. This type of dynamics is shown in Fig. 8A for the oscillator with no aperture inside the cavity. The steady state is characterized by irregular variations in the oscillation wave intensity.

With the 0.5-mm aperture introduced into the cavity, only one transverse mode is oscillating. Its temporal dynamics is either smooth, as shown in Fig. 8B, or features periodic variations (Fig. 8C). The periodic modulation usually occurs for a smaller imbalance of pump intensities; it disappears if the backward pump-wave intensity becomes much smaller than that of the forward pump wave.

To check that the observed dynamics in Fig. 8C is an inherent feature of the studied photorefractive oscillator and not an artifact, the intensity dependence of the modulation frequency has been measured (Fig. 9). This dependence is nearly linear, as one can expect by taking into account that the space-charge relaxation rate is governed by photoconductivity. In fact, because of sublinear intensity

dependence of photoconductivity, $\sigma = \kappa I^x$, typical for crystals with shallow traps,[19] the measured intensity dependence of the beat frequency is better fitted by $\Omega \propto I^x$ dependence. The exponent x extracted from this fit, $x = 0.83$, is the same as that already reported for our sample in a previous publication.[20]

The high-contrast nearly harmonic modulation of the oscillation intensity in Fig. 8C results from the simultaneous excitation of two longitudinal modes with different frequencies. To prove that these two frequencies are shifted symmetrically with respect to the pump frequency, the coherent reference wave is sent to the detector along with the oscillation wave. Figure 10 shows how the modulation frequency is changing if the reference wave is

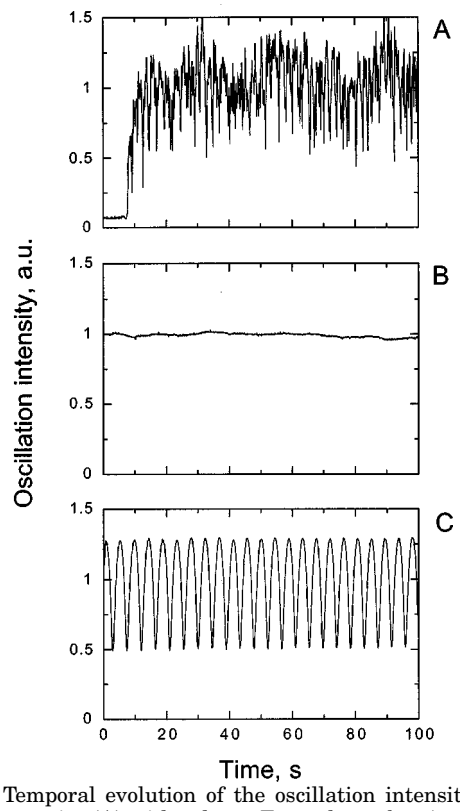

Fig. 8. Temporal evolution of the oscillation intensity for the semilinear cavity (A) with a large Fresnel number (no aperture inside the cavity) and (B,C) with a 0.5-mm aperture inside. The cavity mirror reflectivity is $R = 1$, the pump ratio $r = 200$ for (B), and $r = 20$ for (C).

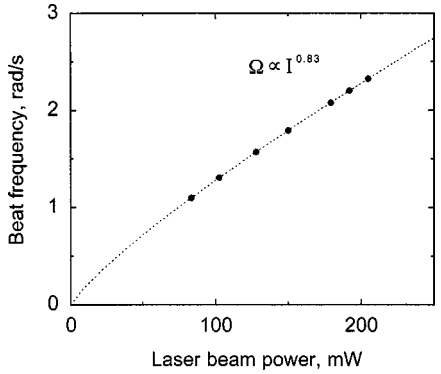

Fig. 9. Beat frequency in the oscillation wave versus laser pump power. The dashed curve is the fit to I^x dependence.

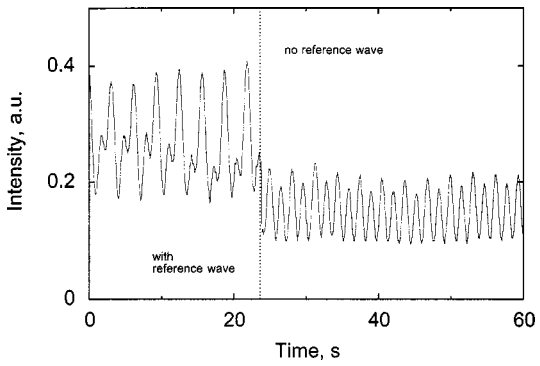

Fig. 10. Temporal intensity variations for the oscillation wave plus a coherent reference wave from the Ar^+-laser and intensity variations of the oscillation wave only.

added or removed. In case the reference wave is present, the most pronounced beat frequency is two times smaller than without the reference wave. This is just what was expected: Without the reference wave, two components in the oscillation spectrum with the frequencies $\omega \pm \Omega$ give the beat frequency 2Ω. With the strong reference wave with frequency ω, the main beat frequency becomes Ω. This is confirmed also directly by the Fourier spectra of the relevant signals.

The oscillation dynamics is measured here for different pump-intensity ratios r. Typical examples of pump-ratio dependences of the averaged oscillation intensity and modulation frequency are shown in Fig. 11. These dependences agree well with that predicted by calculations (see Fig. 4). Within the whole interval of r where the oscillation occurs, there are two well separated regions, one with a single-frequency oscillation (large values of r) and another with a two-frequency oscillation.

The largest oscillation intensity is observed roughly near the transition point between the single-frequency and two-frequency domains; it is decreasing gradually both for increasing and decreasing r. This reflects the pump-ratio dependence of the threshold-coupling strength shown in Fig. 4A: The largest oscillation intensity corresponds to the largest difference between the coupling strength that is ensured by the sample and the calculated threshold-coupling strength (similar to conventional lasers where the output intensity is proportional to the overthreshold pump intensity). One can see from Fig. 4 that, for the pump-ratio range of interest, the position of the minimum of threshold coupling strength is rather close to the position of the transition point. The oscillation intensity drops when the threshold coupling strength is approaching the sample coupling strength. The measured pump-ratio dependence of the beat frequency (Fig. 11B) resembles that calculated (Fig. 4B).

Next, the dependence of the oscillation frequency versus the pump ratio is measured more carefully near the transition point. The results are presented in Fig. 12 by dots in a semilog plot that allows showing explicitly the bifurcation. The same figure represents three curves calculated for $R = 1$, 0.1, and 0.01, shown in gray. The observed behavior is qualitatively similar to that predicted by calculations. The frequency splitting occurs at a well-defined pump ratio, and the frequency shift is increasing from zero gradually. At the same time, the experimental

curve measured for a high-reflecting cavity mirror, $R = 1$, is much closer to that calculated for $R = 0.1$. This discrepancy can be attributed in part to other cavity losses not taken into account in calculation (such as losses related to two Fresnel reflections from the sample face at every round trip, diffraction losses because of a small cavity Fresnel number, effective losses because of incomplete overlap of oscillation, and pump waves inside the sample).

It should be emphasized that the comparison with calculation can be only qualitative here. This is because we measure the oscillation frequency for a well developed oscillation, sometimes for pump ratios where coupling strength of the sample is far above the threshold value and the calculation is performed in the undepleted-pump approximation, i.e., always in the vicinity of the transition point. Keeping this in mind, we can state a quite reasonable agreement of the measured and the calculated data.

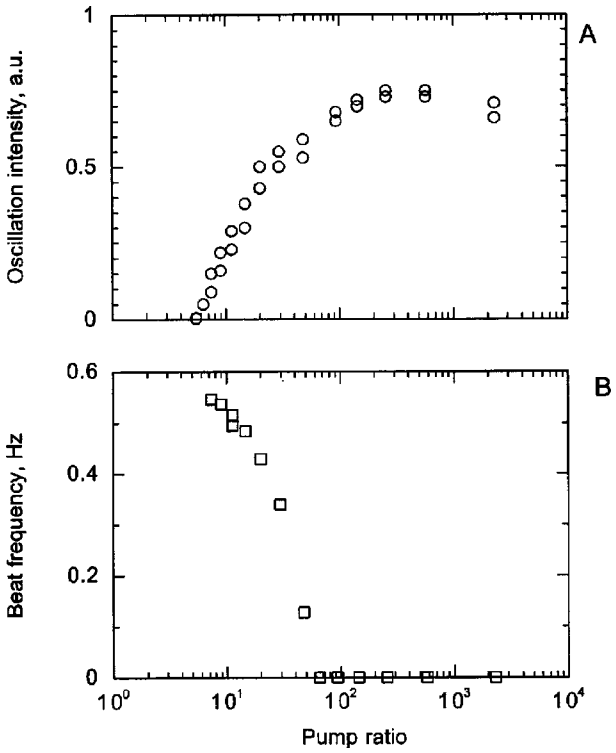

Fig. 11. Pump-ratio dependences of (A) oscillation intensity and (B) modulation frequency.

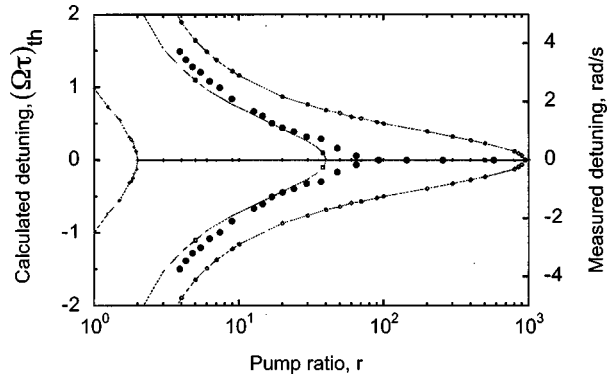

Fig. 12. Oscillation frequency versus pump-intensity ratio. The measured values are shown by filled dots. Solid gray curves represent the results of calculation (see text).

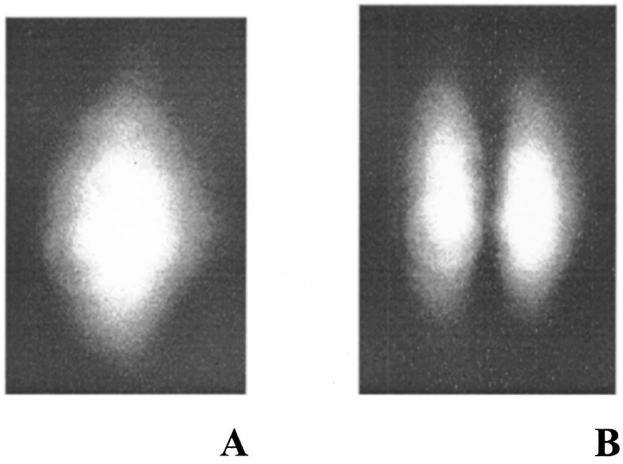

Fig. 13. Far-field intensity distribution for double-frequency oscillation, recorded (A) at maximum and (B) minimum of periodic intensity variations.

The angular distribution of the oscillation wave has been studied, too. Within the pump-ratio range where a single-frequency oscillation is observed, the far-field intensity distribution is bell shaped (Fig. 13A), close to the Gaussian distribution of a TEM_{00} mode of the cavity. For a two-frequency oscillation, the bell-shaped intensity distribution can be observed also, but quite often the periodic appearance of a deep-black fringe is visible (see Fig. 13B) The contrast of this fringe becames the largest every time the periodically modulated oscillation intensity (shown in Fig. 8C) reaches its minimum. At the maxima of the intensity modulation, the intensity distribution remains bell shaped.

It might be thought that two low-transverse-index cavity modes are oscillating simultaneously as it was suggested in Ref. 6. We believe, however, that the observed behavior is not due to the interference of TEM_{00} and TEM_{01} (or TEM_{02}) oscillation modes. Simultaneous excitation of TEM_{00} and TEM_{01} modes usually results in characteristic dynamics of the far-field pattern with periodic out-of-phase modulation of the intensity in two lobes ("dancing modes"[21,22]). From the other side, every cavity eigenmode possesses by definition its own eigenfrequency. This presumes that, when the reference beam from an Ar^+-laser interferes with the two-lobe oscillation mode, the light fringes are either stable in time (two waves with the same frequency) or move in the same direction (the same frequency shift for both lobes of eigenmode).

A qualitatively different behavior is observed experimentally: The symmetric two-lobe pattern is alternating with a bell-shaped pattern (Fig. 13), and no out-of-phase modulation in two lobes occurs. Furthermore, the interference fringes shown in Fig. 14 are moving in opposite directions in the two lobes of the far-field pattern. Two immobile opaque markers placed on the white screen (in the right-hand top corner and in the left-hand bottom corner of the patterns shown in Fig. 14) allow detecting opposite directions of the fringes motion in two lobes.

This motion results in fringe discontinuity within the far-field light spot. The fringe pattern becomes uniform

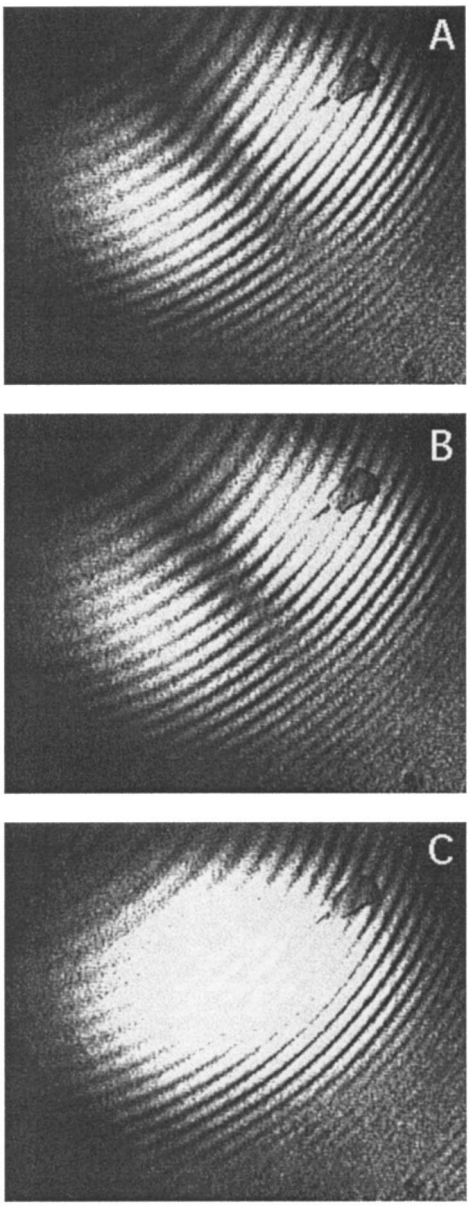

Fig. 14. Fringe pattern of far-field intensity distribution for two-frequency oscillation and Gaussian reference beam from an Ar^+ laser. Consecutive frames A and B show clearly the switch of interlinks between the fringes in two bright areas, which is due to the fringe motion in opposite directions. Markers on the screen allow the detection of the fringe-motion directions.

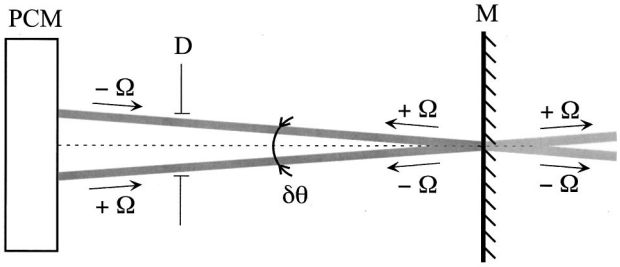

Fig. 15. Schematic representation of tilted rays in the cavity with the phase-conjugate mirror (see text).

throughout a whole bright spot (Fig. 14A) only at the maxima of oscillation intensity. Figures 14A and 14B show two consecutive snapshots (taken from a movie recorded with a CCD camera) near the minimum of the oscillation intensity, when the fringes in two lobes are nearly out of phase. The abrupt switching of interlinks between two sets of fringes for exactly one fringe spacing is obvious; it results from contradirectional fringe motions in two lobes.

Such a behavior is typical for an oscillation wave that consists of two components, oppositely shifted in frequency and making a small angle ($\simeq 10^{-3}$ rad) between them. This behavior can be explained if we assume the excitation of a mode with the rays structure shown in Fig. 15. Two partially overlapping areas in the phase-conjugate mirror are postulated that "reflect" the incident slightly tilted wave exactly in the back direction and change the sign of the frequency detuning to the opposite. An argument in favor of this explanation is the observation of up to three moving black fringes in the far-field pattern for the coherent oscillator with a larger aperture (1 mm) inside the cavity. The excitation of these modes may be a consequence of an inexact angular alignment of the two counterpropagating pump waves. It may be related to a nonlinear phase mismatch in this four-wave interaction coming from the frequency shift of the oscillation waves. It is known that such a phase mismatch might be compensated for by the angular misalignment.[14]

C. Mirrorless Oscillation

Several types of coherent mirrorless oscillation have been reported for different parametric mixing processes in $BaTiO_3$ crystals,[23,24] but, surprisingly, the most simple one that is due to backward four wave mixing[1,3] has not been yet observed, to our knowledge. Most probably, this is because the researchers are using in their experiments

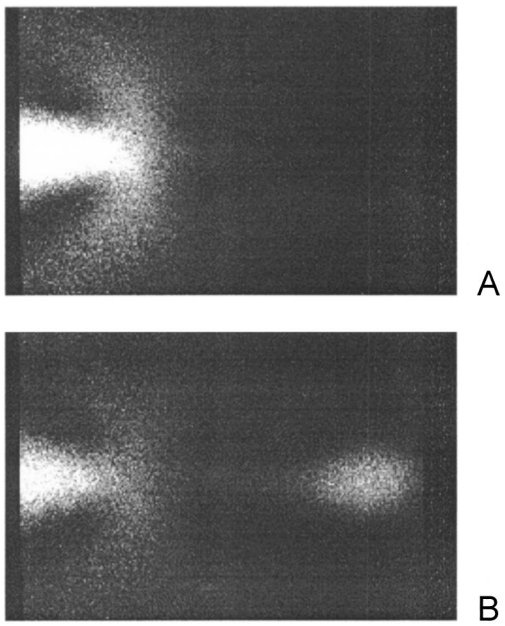

Fig. 16. Angular distribution of (A) light-induced scattering and (B) light-induced scattering with mirrorless oscillation.

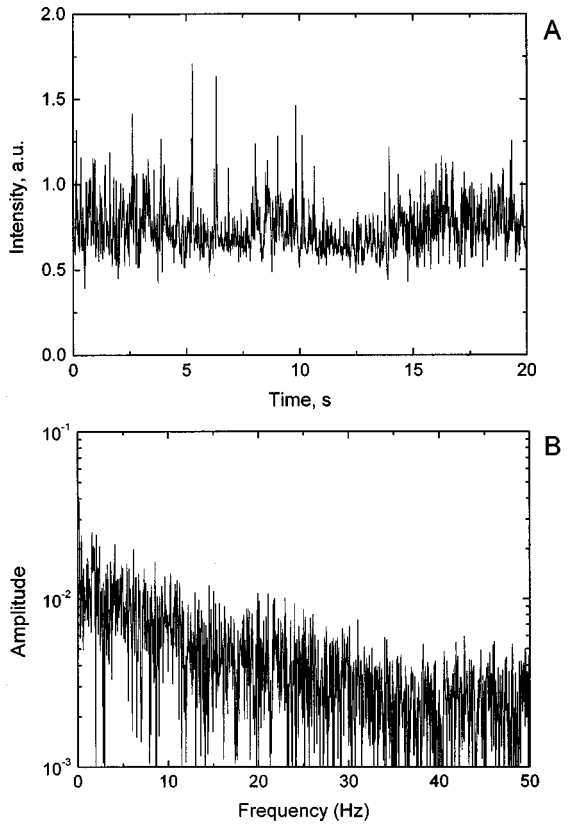

Fig. 17. (A) Temporal variations of the mirrorless oscillation intensity and (B) their corresponding Fourier spectrum.

quite moderate coupling strength, $\gamma_0 \ell \simeq (2 \ldots 3)$, which is not sufficient for a self-excitation of mirrorless oscillation.

If no other restrictions are imposed, the angular distribution of the oscillating wave(s) should reflect the angular distribution of the gain factor (i.e., the angular dependence of the coupling strength). So the oscillation within a rather wide angular window could be expected, roughly corresponding to the angular distribution of the light-induced scattering but with better-defined edges and much stronger intensity.

Experimentally, it is easier to detect the self-development of mirrorless oscillation by observing it in a direction where it is not masked by the scattered light. Figure 16A shows the angular distribution of the scattered light copropagating with the forward (more intense) pump wave. It has the characteristic shape of a cross centered in the direction of the crystal polar axis.[25,26] The right-hand side ray of the cross is absent because of a much smaller gain factor for this direction: scattered light is not amplified sufficiently. Whenever the mirrorless self-oscillation occurs, it propagates both in the brightest left ray of the scattering cross and also in the opposite direction. This backpropagating oscillation wave is reflected by the sample face close to the beam splitter (see Fig. 7) in the direction of the missing right ray of the cross (Fig. 16B).

According to the calculation presented above, the mirrorless oscillation can never occur with the same frequency as that of the pump waves (the dashed curve in Fig. 4B does not intersect abscissa for any finite r). The dynamics of the intensity variation of the observed mirrorless oscillation is not smooth but exhibits pronounced irregular oscillations (Fig. 17A). The Fourier spectrum of this signal features a long tail slowly decreasing with the temporal frequency (Fig. 17B). This corresponds to excitation of a large number of modes with different eigenfrequencies, which is not astonishing, taking into account that the sample coupling strength is larger than the smallest threshold coupling strength 2π and threshold condition can be satisfied, in principle, within a rather wide range of detuning frequencies.

Qualitatively, the observed features do not contradict the expected ones for mirrorless oscillation, which is due to backward-wave four-wave mixing with the dominant transmission gratings. At the same time, additional proof is necessary to make an unambiguous conclusion about the nature of the observed mirrorless oscillation.

5. DISCUSSION

From the comparison of the experimental data and the results of calculation, one can state the satisfactory agreement between them. The two-frequency oscillation is predicted for semilinear oscillator with the external mirror and observed experimentally with the properties close to expected ones.

It would be interesting to compare the reasons for multifrequency oscillation in conventional lasers and in photorefractive oscillators. In lasers with nondispersive cavities (cavity losses independent of frequency), the origin of multifrequency oscillation is usually related to different kinds of inhomogeneity, which results in the possibility for different (weakly interacting or noninteracting) spectral components to reach the threshold independently.[27] The inhomogeneity might be spatial: modes of the Fabry–Perot cavity with different indices have different spatial structures and therefore get amplified in incompletely overlapping areas of the active medium, thus leading to spatial hole burning.[28] It may be also spectral: The ultimate case is the gas laser, where different longitudinal modes are fed by different components of the Doppler-broadened gain spectrum.[28] The solid-state lasers with inhomogeneously broadened gain spectra (such as Nd^{3+}-glass lasers) are good examples, too.[29,30] And, finally, the polarization inhomogeneity may also become a reason of multifrequency oscillation.[31]

In photorefractive oscillators, a double-frequency oscillation can also result from inhomogeneity: it may be caused by the simultaneous formation of two space-charge gratings by the carriers with different charges, such as in $Sn_2S_2P_6$.[32] In such a material, the gain spectrum itself has a two-maxima profile, and the oscillation is nondegenerate for all possible configurations of optical oscillators.

The onset of multifrequency oscillation occurs in different ways in all these cases. The single-mode oscillation at the threshold can be transformed either in multimode oscillation with a continuous spectrum (spatial hole burning and spectral hole burning in gas lasers[28]) or split into two (and later, maybe, into three and four) spectral components (spectral hole burning in Nd^{3+} glasses,[29,30] splitting of one mode in gas lasers into two with different

polarizations[31]). In a formal way, the frequency bifurcation in the considered photorefractive oscillator is closer to the two last-mentioned conventional lasers. The reason for a frequency split is, however, completely different from usual lasers, as no type of inhomogeneity is considered for a photorefractive oscillator. The transformation of the phase-conjugate reflectivity spectrum from a one-maximum to a two-maxima profile occurs rather because of competition of two contributions to four-wave mixing gain, one from the local and the other from the nonlocal nonlinear response.

ACKNOWLEDGMENTS

The authors are grateful to P. Jullien and A. Shumelyuk for stimulating discussions and to G. Pauliat for a Faraday isolator. S. Odoulov is thankful to colleagues from Laboratoire de Physique, Université de Bourgogne, for their hospitality during his stay as an invited professor in Dijon.

D. Rytz can be reached by e-mail at rytz@fee-io.de. P. Mathey can be reached by e-mail at pmathey @u-bourgogne.fr.

REFERENCES

1. A. Yariv and D. Pepper, "Amplified reflection, phase conjugation, and oscillation in degenerate four-wave mixing," Opt. Lett. **1**, 16–18 (1977).
2. J. Feinberg and R. Hellwarth, "Phase conjugate mirror with continuous wave gain," Opt. Lett. **5**, 519–521 (1980).
3. M. Cronin-Golomb, B. Fischer, J. O. White, and A. Yariv, "Theory and applications of four-wave mixing in photorefractive media," IEEE J. Quantum Electron. **QE-20**, 12–30 (1984).
4. A. A. Bagan, V. B. Gerasimov, A. V. Golyanov, V. E. Ogluzdin, V. A. Sugrobov, I. L. Rubtsova, and A. I. Khyzhnjak, "Conditions for the stimulated emission from a laser with cavities coupled via a dynamic hologram," Sov. J. Quantum Electron. **17**, 49–51 (1990).
5. G. C. Valley and G. J. Dunning, "Observation of optical chaos in a phase conjugate resonator," Opt. Lett. **9**, 513–515 (1984).
6. Siuying R. Liu and G. Indebetouw, "Periodic and chaotic spatiotemporal states in a phase-conjugate resonator using a photorefractive $BaTiO_3$ phase-conjugate mirror," J. Opt. Soc. Am. B **9**, 1507–1520 (1992).
7. P. Mathey, P. Jullien, S. Odoulov, and O. Shinkarenko, "Manifestation of optical Curie–Weiss law for optical phase transition," Appl. Phys. B **73**, 711–715 (2001).
8. P. Mathey, P. Jullien, S. Odoulov, and O. Shinkarenko, "Second-order optical phase transition in a semilinear photorefractive oscillator with two counterpropagating pump waves," J. Opt. Soc. Am. B **19**, 405–411 (2002).
9. M. G. Reznikov and A. I. Khizhnyak, "Properties of a resonator with a wavefront reversing mirror," Sov. J. Quantum Electron. **10**, 533–634 (1979).
10. P. A. Belanger, A. Hardy, and A. Siegman, "Resonant modes of optical cavities with phase-conjugate mirrors," Appl. Opt. **19**, 602–609 (1980).
11. G. Nicolis, *Introduction to Nonlinear Science* (Cambridge University, New York, 1995).
12. M. C. Cross and P. C. Hohenberg, "Pattern formation outside of equilibrium," Rev. Mod. Phys. **65**, 851–1112 (1993).
13. K. R. McDonald and J. Feinberg, "Enhanced four-wave mixing by use of frequency shifted waves in photorefractive $BaTiO_3$," Phys. Rev. Lett. **55**, 821–824 (1985).
14. S. Odoulov, M. Soskin, and A. Khyzhnyak, *Optical Coherent Oscillators with Degenerate Four-Wave Mixing (Dynamic Grating Lasers)* (Harwood Academic, Chur, Switzerland, 1991), pp. 37–39.
15. J. Feinberg, "Self-pumped, continuous-wave phase conjugator using internal reflection," Opt. Lett. **7**, 486–488 (1982).
16. Y. Feinman, E. Klancnik, and S. H. Lee, "Optimal coherent image amplification by two-wave coupling in photorefractive $BaTiO_3$," Opt. Eng. **25**, 228–234 (1886).
17. D. Engin, S. Orlov, M. Segev, G. Valley, and A. Yariv, "Order-disorder phase transition and critical slowing down in photorefractive self-oscillators," Phys. Rev. Lett. **74**, 1743–1746 (1995).
18. M. Goul'kov, O. Shinkarenko, S. Odoulov, E. Kraetzig, and R. Pankrath, "Threshold of oscillation in a ring-loop phase conjugator as a second order optical phase transition," Appl. Phys. B **72**, 187–190 (2001).
19. D. Mahgerefteh and J. Feinberg, "Explanation of the apparent sublinear photoconductivity of photorefractive barium titanate," Phys. Rev. Lett. **64**, 2195–2198 (1990).
20. P. Mathey, B. Mazué, P. Jullien, and D. Rytz, "Dynamics of optical filtering and edge enhancement in cobalt-doped barium titanate," J. Opt. Soc. Am. B **15**, 1353–1361 (1998).
21. J. P. Jiang and J. Feinberg, "Dancing modes and frequency shifts in a phase conjugator," Opt. Lett. **12**, 266–268 (1987).
22. A. Mazur and S. Odoulov, "Ring photorefractive oscillator with linear cavity distortion," IEEE J. Quantum Electron. **26**, 963–966 (1990).
23. S. Odoulov, U. van Olfen, and E. Kraetzig, "Mirrorless parametric oscillation in $BaTiO_3$," Appl. Phys. B **54**, 313–317 (1992).
24. B. Sturman, S. Odoulov, and M. Goul'kov, "Parametric four-wave processes in photorefractive crystals," Phys. Rep. **275**, 197–254 (1996).
25. R. Grousson, S. Mallick, and S. Odoulov, "Amplified backward scattering in $LiNbO_3$:Fe," Opt. Commun. **51**, 342–346 (1984).
26. D. Dolfi, A. Delboulbe, and J.-P. Huignard, "Forward mixing of two mutually incoherent beams in a photorefractive crystal," Electron. Lett. **29**, 450–451 (1993).
27. A. Yariv, *Quantum Electronics* (Wiley, New York, 1989).
28. A. E. Siegman, *Lasers* (University Science, Mill Valley, Calif., 1986).
29. V. S. Mashkievich, "Theory of laser kinetics for systems with inhomogeneously broadened luminescence spectra," Ukr. Phys. J. **12**, 1731–1736 (1967).
30. A. D. Manuilskii, S. G. Odoulov, and M. S. Soskin, "Homogeneous linewidth determination for disordered active media from stimulated emission spectra of internal modes," Phys. Status Solidi **35**, k111–k113 (1969).
31. O. Emile, M. Brunel, A. Le Floch, and F. Bretenaker, "Vectorial excess noise factor in common lasers," Europhys. Lett. **43**, 153–157 (1998).
32. A. Shumelyuk, S. Odoulov, and G. Brost, "Multiline coherent oscillation in photorefractive crystals with two species of movable carriers," Appl. Phys. B **68**, 959–966 (1999).